International Journal of Pharmacology

ISSN 1811-7775

science alert

ansinet
Asian Network for Scientific Information

OPEN ACCESS International Journal of Pharmacology

ISSN 1811-7775
DOI: 10.3923/ijp.2016.304.316

Research Article
Role of Anti-apoptotic Activity of Antioxidants in Conferring Protection Against Prostate Cancer

[1,2]Peijie Chen, [2]Peiming Bai, [2]Guangcheng Luo, [2]Hanzhong Su, [2]Ruixiong Shen, [2]Ziming Liu, [2]Nangen Zhang, [2]Lin Fang and [1]Chunxiao Liu

[1]Department of Urology, Zhujiang Hospital, Southern Medical University, Guangzhou 510280, China
[2]Department of Urology, Zhongshan Hospital Xiamen University, Xiamen 361004, China

Abstract
The drug delivery potential of lipid and polymer based nano-carriers to achieving greater drug bioavailability has driven a renewed interest in their uptake mechanisms employed and movement within cells. Therefore, present study was designed to formulate resveratrol (Res) loaded Solid Lipid Nanoparticles (SLNs) as novel prototypes for prostate cancer treatment, to characterize and to assess the targeted and controlled delivery attributes of SLNs in human prostate cancer cells. The SLNs were prepared by a solvent diffusion evaporation method and characterized with respect to morphology, particle size and zeta potential, encapsulation and loading efficiency and *in vitro* release studies. Further, various process parameters were optimized for Res-loaded SLNs to obtain higher drug loading and entrapment efficiency with less than 200 nm uniform dispersity. The effects of free resveratrol (Res) and Res loaded SLNs (Res-SLNs) on internalization, cell uptake, viability, nucleosomal morphology, DNA fragmentation and Bcl-2 level was evaluated and compared with free Res on prostate cancer cells (PC-3). The immunofluorescence assay suggests that SLNs with a size lower than 175 nm showed rapid movement through cell membrane, distributes throughout the cytosol and moves successively among different cellular levels with minimal and acceptable cytotoxicity. The release profile of Res showed a bi-phasic pattern, showing its distribution in SLNs. The Res in solution was seen slightly cytotoxic and cytotoxicity was increased after encapsulating it in SLNs. Collectively, delivery of Res through SLNs contributes to effectiveness of Res on decreasing cell proliferation, with potential of inducing selective apoptosis of prostate cancer.

Key words: Prostate cancer, solid lipid nanoparticles, resveratrol, apoptosis, oxidative stress

Received: December 02, 2015 **Accepted:** February 10, 2016 **Published:** April 15, 2016

Citation: Peijie Chen, Peiming Bai, Guangcheng Luo, Hanzhong Su, Ruixiong Shen, Ziming Liu, Nangen Zhang, Lin Fang and Chunxiao Liu, 2016. Role of anti-apoptotic activity of antioxidants in conferring protection against prostate cancer. Int. J. Pharmacol., 12: 304-316.

Corresponding Author: Chunxiao Liu, Department of Urology, Zhujiang Hospital, Southern Medical University, No. 253 Middle of Industry Avenue, Guangzhou City, China Tel/Fax: 0086-020-61643888

Competing Interest: The authors have declared that no competing interest exists.

Data Availability: All relevant data are within the paper and its supporting information files.

INTRODUCTION

Prostate Cancer (PC) is the most commonly diagnosed solid malignancy and second leading cause of cancer-related mortality in the population living in developed countries (Pathak *et al*., 2005). It is evident and apparent from the studies carried out that predisposing factors for prostate cancer condition are the androgens, genetic susceptibility and environmental exposures, such as diet (dietary fat and low anti-oxidant compounds) play a crucial role in in prostatic carcinogenesis (Fleshner and Klotz, 1998). Above-stated risk factors eventually lead to generation of oxidative stress and free radicals within prostatic cells. The oxidative stress is the crucial player for the initiation and development of prostate cancer pathology (Lin *et al*., 2010; Alqahtani and Kaddoumi, 2015; Antwi *et al*., 2015). The impaired balance between production and clearance of Reactive Oxygen Species (ROS) or Reactive Nitrogen Species (RNS) may result into prostate cancer pathology. Reactive Oxygen Species (ROS), such as hydrogen peroxide (H_2O_2), superoxide anion radical (O_2) and the hydroxyl radical ($OH^•$) is an entire class of highly reactive molecules derived from metabolism of oxygen. The ionizing radiations and chemicals (Garcia-Ruiz *et al*., 1995) have been used in many human degenerative diseases, such as ageing, cancer, Huntington's disease, cardiovascular disease, mutations and neurodegenerative ailments, Alzheimer's and Parkinson's (Finkel and Holbrook, 2000). The H_2O_2 is known to modulate diverse cellular functions *in vivo* by producing hydroxyl radicals by DNA and metal ions interaction. Hydrogen peroxide induces DNA and cell damage by lipid peroxidation (Ueda and Shah, 1992). The apoptosis and necrosis have different impacts on cellular physiology, the cellular response to H_2O_2 is in continuum from apoptosis to necrosis (Gardner *et al*., 1997) i.e., high concentration leads the cells to be necrotic and converse is applicable to apoptosis (Lennon *et al*., 1991). The antioxidant defense system of our body including glutathione, superoxide dismutase and catalase, renders protection against oxidative stress (Mohanty *et al*., 2014).

Antioxidants are very useful for chemoprophylaxis of prostate cancer by evoking immune and regulate the production of free radicals. The super-oxide (antioxidant) gets accumulated in ageing body and plays an important role in causing prostate cancer pathogenesis (Torricelli *et al*., 2011). The supplementary antioxidants can be exogenously obtained from animal and plant sources; however, those obtained from plant origin are of enormous interest due to their easy availability and potent antioxidant activity (Carlsen *et al*., 2010). The relevance of antioxidants is surfaced by the study reported earlier (La Vecchia *et al*., 2001), which suggested that persons consuming diet rich in fruits and vegetables are less prone to developing cancer.

Resveratrol (3,4 ,5-trihydroxy-trans-stilbene) is one such poly-phenolic antioxidant, common constituent of red wine and has been detected in more than 70 plant species (Johnson *et al*., 1994) and is reported to possess many biological activities for human cancer treatment (Bishayee, 2009). There are very recent reports, which have reportedly shown usefulness of resveratrol in preventing and treating prostate cancer (Fraser *et al*., 2014; Mitani *et al*., 2014; Empl *et al*., 2015). Apoptosis is an active cell death mechanism, which occurs during cancer pathologies (Kobori *et al*., 1999; Wang *et al*., 1999; Iwashita *et al*., 2000). There are two underlying pathways to induce apoptosis; death-receptor and mitochondrial pathway mediated by caspase-8 and caspase-9, respectively. Eventually, both pathways converge to activate effecter caspase-3 (Chandra *et al*., 2000; Zimmermann *et al*., 2001; Cain *et al*., 2002; Mathiasen and Jaattela, 2002) to induce programmed cell death. Pro-apoptotic (bax) and anti-apoptotic (bcl-family) differential expression determines the inherent susceptibility of cells that respond to apoptotic signals. The bax and bcl-2 are crucial proteins of bcl-2 family and ratio of bcl-2/bax plays an instrumental role in the regulation of apoptosis (Tjalma *et al*., 2001).

The present study exploit the therapeutic potential of resveratrol in conferring robust immunity against prostate cancer. However, effective delivery of resveratrol to the targeted sites has been a challenge due to poor solubility, instability and poor bioavailability due to its extensive metabolism in liver and intestine (Walle, 2011). Thus, there is an increasing need to use novel drug delivery systems, such as Solid Lipid Nanoparticles (SLNs) to deliver antioxidants. They are an emerging drug delivery system due to their advantages over others such as low cost, ease of production, biocompatibility, non-immunogenicity, targeted and sustained delivery. This study is designed to evaluate anti-cancer and anti-apoptotic activities of resveratrol in prostate cancer cells (PC-3). Further, resveratrol loaded onto solid lipid nanoparticles have shown the improved bioavailability, efficacy and therapeutic potential in treating prostate cancer.

MATERIALS AND METHODS

Chemicals: Trans-resveratrol (RSV, >99% pure) was procured from Sigma, Germany. Solid lipids Stearic Acid (SA) and tristearin were purchased from Qingdao Huatuo Chemicals Co., Ltd. Phospholipid 90G was obtained as gift sample from Lipoid, Germany. All other chemicals were of analytical grade and purchased from local vendors.

Preparation of resveratrol loaded SLNs (Res-SLN): Resveratrol loaded SLNs were prepared by solvent diffusion evaporation method. Briefly weighed amount of drug and solid lipid mixture (SA: tristearin) with phospholipid 90 G 1:1 was dissolved in 6 mL of acetone:ethanol (1:1) mixture by heating at 60-70°C. The heated organic phase was mixed drop to drop into aqueous phase (1% tween 80) solution containing Dextran Sulfate (DS) on the constant magnetic stirring. The organic phase was then allowed to evaporate for 5-6 h at ambient temperature. The lipidic nano-suspension was centrifuged at 20,000 rpm for 1 h to separate nanoparticles. The obtained pellet was washed twice with distilled water and suspension was centrifuged. Various process variables for the preparation of SLNs were optimized to acquire a final formulation with small particle size (<200 nm), narrow Poly-Dispersity Index ((PDI), <0.5) and maximum drug loading with high entrapment efficiency (>70%). The final washing of the pellet followed the dispersion of it in minimum amount of water to be lyophilized.

Characterization of Res-SLNs

Size, PDI and surface morphology: The size and polydispersity index (PDI) of SLNs was determined with Malvern Zetasizer (Malvern Zetasizer, UK). Briefly, small amount of nano-suspensions was diluted 10-20 times and put in the capillary cell for measurement of size and PDI.

The surface morphology of SLNs was assessed by Transmission Electron Microscopy (TEM). In brief, a drop of SLN dispersion was placed onto a copper grid and stained with 1% (w/v) of phosphotungstic acid (PTA) and grid was kept immovable to get the drop dry. The grid was then loaded on JEOL microscope for imaging and analysis was carried out.

Drug entrapment efficiency: Drug entrapment efficiency of SLNs was determined by direct lysis method. Briefly, weighed amount of lyophilized pellet was dissolved in 5 mL of chloroform. The lysate was then centrifuged at 10,000 rpm for 5 min and supernatant was charged into HPLC for the estimation of drug content. The percentage drug encapsulation efficiency (% EE) and drug loading were calculated by the equation:

$$\text{Entrapment efficiency (\%)} = \frac{\text{Amount of drug in SLNs}}{\text{Total amount of drug added}} \times 100$$

$$\text{Drug loading (\%)} = \frac{\text{Amount of drug entrapped in SLNs}}{\text{Total amount of lipid in SLNs}} \times 100$$

Quantification of resveratrol by HPLC method: The resveratrol was quantified on HPLC system (Shimatzu, Japan), which consists of UV detector. The HPLC analyses were performed on Inertsil ODS-3 C18 (5 µm, 250×4.6 mm) column. The mobile phase comprises acetonitrile and ammonium acetate buffer (pH 3.5) with the ratio of 37:63, was kept in an isocratic mode. The flow rate was kept at 1 mL min^{-1} to quantify resveratrol at 306 nm.

***In vitro* drug release:** The *in vitro* drug release study was performed in PBS (pH = 7.4) by using dialysis bag method. Briefly, a known amount of lyophilized SLN was dispersed in 2 mL release medium and put into dialysis bag. This dialysis bag then immersed in 20 mL release medium. After specific time intervals, 0.5 mL sample was withdrawn and replaced with the same medium to maintain the sink conditions. The time points for sampling were 15 and 30 min and 1, 2, 3, 4, 6, 24 and 48 h.

Cell viability assessment: The cell viability was assessed by 3-(4,5-dimethylthiazol-2yl-)-2,5-diphenyl tetrazolium bromide (MTT) method. This method is based on cleavage of a tetrazolium salt by mitochondrial dehydrogenases in viable cells (Garg *et al*., 2011). Cultured PC-3 cells (2×10^6) were seeded and allowed to adhere in a 96 well plate using RPMI-1640 medium. The cells were treated with free resveratrol and resveratrol-SLNs at 20 µg mL^{-1} resveratrol concentration followed by 2 h incubation and 3.5 mM H_2O_2 was mixed and incubated for another 3 h. After completion of the incubation, 25 µL MTT (5 mg mL^{-1}) reconstituted in PBS was added upon was added to each well and incubated for 4 h at 37°C. The obtained formazan crystals were dissolved in 150 µL DMSO and quantitative estimation of formazan purple by absorbance (at 540 nm) was done. The survival rate (30%) of cells treated with H_2O_2 (with no anti-oxidant) was taken as control and percent viability for treated cells (with anti-oxidant) was expressed with reference to percentage viability of control cells.

Nuclear morphology analysis: The nuclear morphology was observed by Propidium Iodide (PI) test. The PC-3 cells were cultured, seeded on sterilized cover glasses and treated with Res and Res-SLNs (equivalent to 100 µg mL^{-1}), for 24 h and PI staining (10 µg mL^{-1}) was done. The morphology of cell nucleus was observed under fluorescence microscope at 200x magnification with a cell number of 2×10^6 cells (Garg *et al*., 2011).

Detection of nucleosomal DNA damage and fragmentation: Photometric immuno-assay of cytoplasmic histone associated DNA fragments were used to quantitate the estimation of cell death (apoptosis). In brief, PC-3 cells were cultured for 18 h and were exposed to plane (Res) and SLN loaded Res for 3 h. The cells were pelleted and incubated in lysis buffer for 30 min at room temperature and centrifuged at 200×g for 10 min. The mono and oligonucleosomes (released by treated cells) were detected by ELISA from supernatant. The results were expressed in terms of an enrichment factor, i.e., ratio of absorbance (A_{405}/A_{490} nm) of treated cells/absorbance (A_{405}/A_{490} nm) to that of control cells.

The DNA fragmentation was determined by using conventional agarose gel electrophoresis by apoptotic DNA ladder kit, following manufacturer recommendations. In short, PC-3 cells (2×10^6) were lysed with the help of lysis buffer (6M guanidine HCl, 100 mM urea, 10 mM tris-HCl and 20% triton-X-100, pH 4.4), DNA was purified and separated by glass entrapment method in glass fibre fleece and eluted with the help of elution buffer (10 mM tris, pH 8.5). The DNA aliquots (1-3 μg well^{-1}) were prepared and loaded onto 1% agarose gel containing 50 μg of ethidium bromide and were run on electrophoresis assembly at 75 V for 1.5 h. The DNA was visualized by placing the gel over UV-trans-illuminator (Garg *et al*., 2011).

Bcl-2 detection

Protein extraction: The anti-oxidants treated cells were lyzed through sonication method. The cell lysate and ice-chilled methanol (1:4) was mixed and left on ice for 1 h. The pellet comprising protein was collected by the centrifugation at 10,000 rpm for 15 min and suspended in 0.25M tris-HCl buffer (pH 6.8) containing 10 mg mL^{-1} leupeptin, 1 mg mL^{-1} aprotinin and 10 mg mL^{-1} pepstatin. The total protein content was estimated by the method reported by Lowry *et al*. (1951).

Immunoblotting: Sodium dodecyl sulphate polyacrylamide gel electrophoresis (SDS-PAGE) method was used for separation of detergent soluble proteins (40-60 μg protein lane^{-1}) on 10% gel under reducing conditions. Protein solution was mixed with sample buffer and protein concentration was adjusted to 2 μg μL^{-1}. Then, proteins were transferred onto nitrocellulose membrane at 100 V for 2 h. Nitrocellulose membrane was blocked overnight at 4°C with 5% skimmed milk powder in PBS and subsequently incubated for 1 h with rabbit-anti-Bcl-2 monoclonal antibody. The membrane was washed by PBST (0.05% tween-20) and then probed with anti-rabbit-IgG conjugated with alkaline phosphates in 2.5% skimmed milk in PBS for 1 h at 37°C. Finally, membrane was rinsed twice with PBS-T and two times with PBS. Protein bands were visualized by membrane incubation with BCIP-NBT substrate (5-bromo-4-chloro-3-indolyl phosphate-nitro blue tetrazolium). The band intensity of protein was quantitated by imaging densitometer software (Bio-Rad, Model GS-670) against the band intensity of experimental control.

Flow cytometry analysis: The FITC labeled SLNs were prepared adding 3.4×10^{-3} m mol of FITC by keeping other constituent constant. The carboxylic (-COOH) and isothiocyanate (NCS) group of FITC react with amine terminal functionalities of plain SLNs. The PC-3 cultured in RPMI-1640 medium supplemented with 10% foetal bovine serum and viable cells (2×10^6 mL^{-1}) were distributed in 96 well micro plates for 24 h and incubated in 5% CO_2 at 37°C. The medium was removed and cells were washed three times by PBS for complete removal of unentrapped SLN, then FITC labelled formulations were added and plates were incubated for 2 h. The 20 μm 2′, 7′-dichlorofluorescin diacetate (DCFH-DA) was loaded after another 45 min and cells were washed with PBS to remove the DCFH-DA. Further, 3.5 mM H_2O_2 was mixed into the cells and incubated for another 45 min and cells were observed under fluorescent spectrophotometer at λex = 475 nm.

Statistical analysis: The results were expressed as Mean±SD. The data obtained was subjected to Student's t-test for statistical analysis and statistical significance was designated as ($p<0.05$). Multiple comparisons were made using one way analysis of variance (ANOVA) followed by *post hoc* analysis using Tukey's test to determine the significance of the results obtained using Graph pad Instat software.

RESULTS AND DISCUSSION

Preparation of resveratrol loaded solid lipid nanoparticles: The Res-SLNs was fabricated using solvent injection technique that involves intense diffusion of solvent transversely i.e., solvent-lipid phase into the surrounding aqueous phase and evaporation of organic solvent that confers rigidity to lipid particles. The high shear homogenization was used to ensure nano-range of the particles. The pre-emulsion phase was acquired by high speed stirring prior to homogenization. The lipids employed in the formulation of SLNs were first subjected to optimization by varying the ratio of lipid: Phospholipid from 1:0.5-1:2. The prepared formulation was characterized with respect to particle size and PDI.

The formulation with 1:1 lipid/lecithin ratio was chosen for optimization process variables as it showed an optimum size (158.3±4.34 nm) and PDI (0.14) of NPs (Fig. 1a). The SLN formulations showed an increase in the size and PDI with an increase in lecithin concentration except the one that was prepared with lipid: Lecithin (1:1). This might be due to the formation of vesicles because excess of phosphatidyl choline forms bilayers in the lipid vesicles. It was observed that upon increasing the quantity of resveratrol, entrapment efficiency increased up to drug: Lipid ratio of 10:100. Moreover, further increase in drug (Res) concentration of lipid leads to the gradual decrease in entrapment efficiency (Fig. 1b). This could be reasoned because of the saturation of lipid with drug. The greater entrapment efficiency (83.80±1.9%) of Res-SLNs was found at 1% surfactant concentration (Fig. 1c). However, further increase or decrease in surfactant concentration has shown decrease in the entrapment efficiency and increase in PDI (Jain *et al*., 2015). The tween-80 minimizes surface tension between aqueous and organic phase that perhaps allows the configuration of tiny droplets of solvent at the site of solvent administration and causes the decrease in the particle size. Further, tween-80 may also help to stabilize the generated surface and particle aggregation (Jain *et al*., 2015). The SLN formulations showed indifferent effects at varying stirring speed. Particle size has seen a decrease upon increasing the stirring speed, but converse was the case after a defined time period. The varying stirring speed of particles showed variation in drug entrapment efficiency of SLNs (Fig. 1a-e). Moreover, the addition of DS (counter ion) establishes an interaction with drug which was largely regulated by a long range electrostatic forces between ion pairing agent DS and drug. It eventually resulted in an increased drug loading because of greater relative lypophilicity of drug. Despite the presence of DS in SLN formulations, average particle size saw a monotonic decrease. This is explained due to higher amphiphilic properties and reduced interfacial tension between two interfaces (Garg *et al*., 2015; Jain *et al*., 2015).

Characterization of resveratrol loaded solid lipid nanoparticles: The average size of all formulations tested was found in 150-350 nm range (Fig. 1). The component ratio and tween 80 concentration dependent changes (deviation in particle size) also showed an impact on PDI and entrapment efficiency of optimized formulation (Fig. 1). The preparation with average particle size (158.3±3.5 nm) and highest EE (83.8%) was considered as optimized formulation, when compared with other formulations (Table 1). The average particle size of Res-SLNs was found to be lower than 200 nm (Table 1). The shape and size of formulated particles is validated by TEM studies (Fig. 2). Further, the size obtained by TEM are different to the one determined by DLS method. The difference in sizes could be attributed to the fact that TEM reveals morphological size of nanoparticle in the solid state, however, zeta sizer measures the hydrodynamic diameter of nanoparticle in aqueous solutions. The results are consistent with the results reported earlier (Garg *et al*., 2015; Jain *et al*., 2015). The second reason might be due to the operation principal of both the instruments; zeta-sizer measures the average particle size whereas, TEM measures size of each and every individual particles. The PDI lesser than 0.3 observed is indicative of homogeneity SLNs size.

The negative zeta potential of Res-SLNs formulation was possibly because of negative charge of phospholipids distributed at SLN's surface. The higher negative value of zeta potential provides repulsive interaction between SLNs and thereby prevents aggregation of nanoparticles. Also, tween 80 as surfactant is thought to confer stearic stability in order to achieving stable formulation.

The greater entrapment efficiency of Res (83.8±2.3%) and drug loading (12.8±1.1) of Res-SLNs was estimated with 1:1 lecithin/lipid (w/w), 1:10 drug: Lipids ratio (w/w) and 1% surfactant concentration (Table 1). Further, addition of DS forms a drug-polymer complex, which leads to increase the partitioning of drug between both the phases and resulting into higher EE of SLN formulations.

***In vitro* release study:** The Res-SLN formulations showed a biphasic sustained release pattern and an initial burst release viz., >30% of Res was estimated from SLN by the end of 2nd h (Fig. 3). A possible reason that may be accounted is the fast release of drug adsorbed on the surface of SLNs or entrapped in the outermost stratum. Further, the cumulative resveratrol release seen from SLN formulation was estimated to be 81.7±2.86% at the end of 48 h. This sustained and prolonged release demeanor of drug molecules observed was mainly due to diffusion of drug through the lipoid matrix of SLNs.

Table 1: Characterization of resveratrol loaded solid-lipid nanoparticles with respect to particle size, PDI, % drug entrapment and drug loading of the optimized formulation

Formulation code	Surfactant concentration (%)	Particle size (nm)	PDI	Entrapment efficiency (%)	Drug loading (%)
Res-SLNs	1.0	158.3±3.5	0.12	83.8±2.3	12.8±1.1

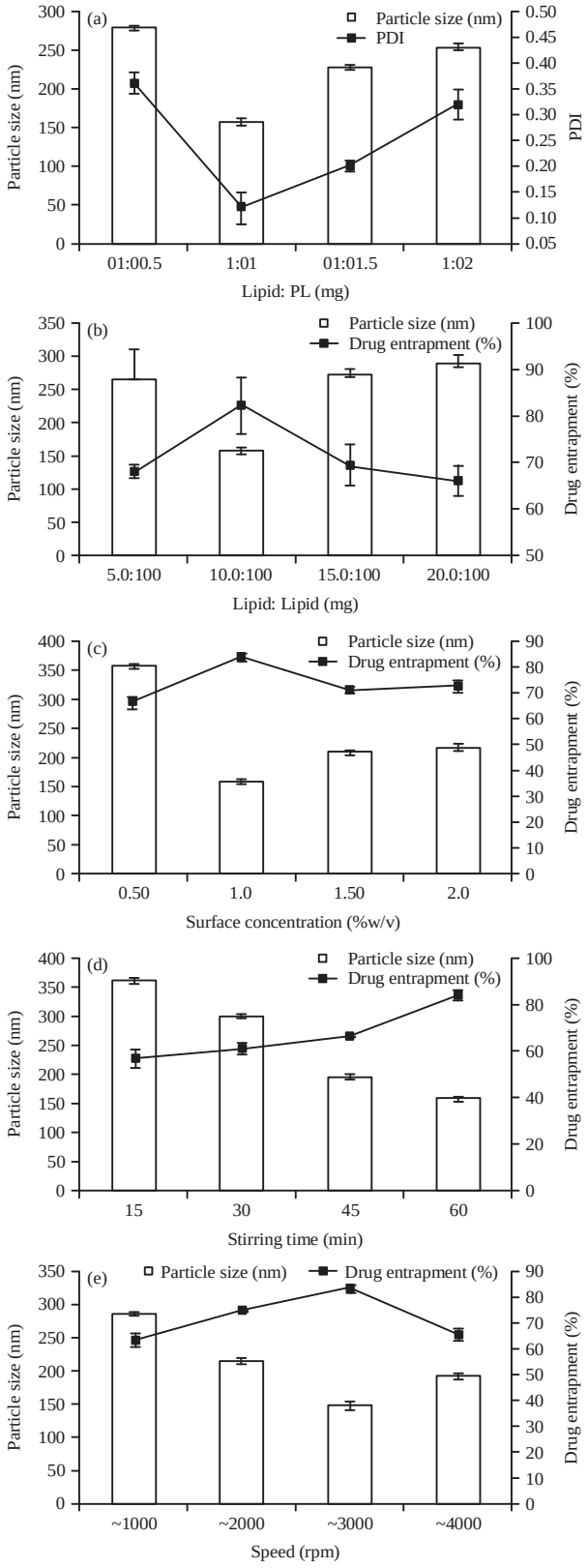

Fig. 1(a-e): Formulation of SLNs and optimization of various process parameters. The optimization of (a) Lipids ratio with respect to particle size, (b) Drug/lipid ratio, (c) Surfactant concentration, (d) Stirring time and (e) Stirring speed with respect to particle size and percentage drug entrapment efficiency (Mean±SD, n = 3)

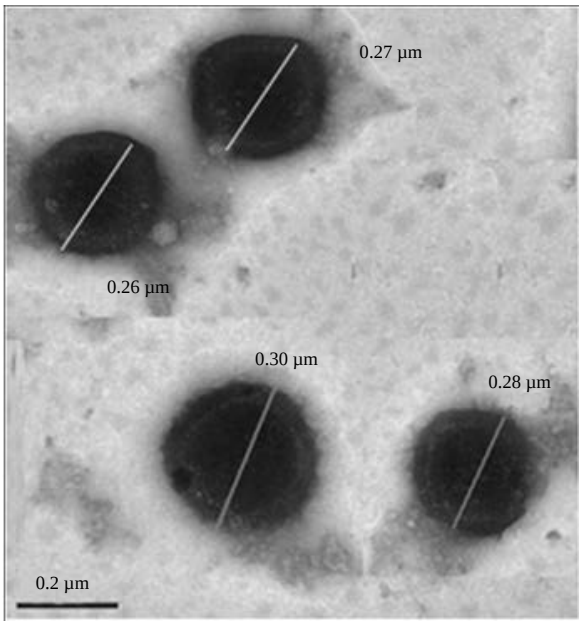

Fig. 2: Phenotypic characterization of resveratrol loaded solid lipid nanoparticles by high resolution-transmission electron microscopy

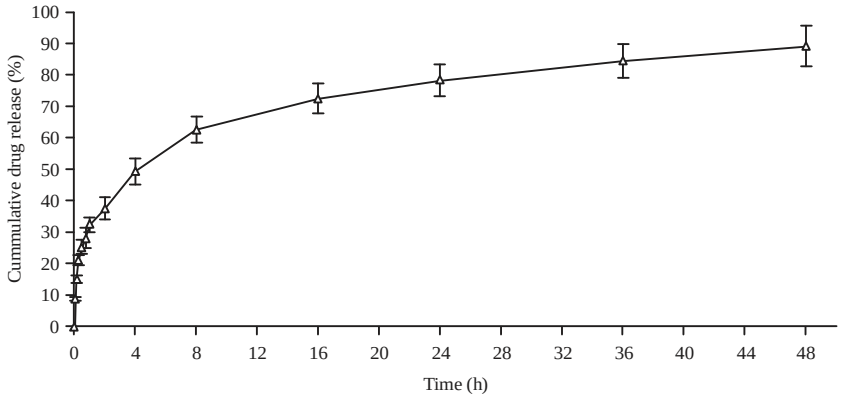

Fig. 3: *In vitro* drug release of resveratrol in physiological PBS (pH 7.4) from SLN formulations (n = 6)

Assessment of cell viability: The cytotoxicity of resveratrol loaded SLNs, free resveratrol and plane SLN (placebo) were tested in PC-3 cells. The results showed that SLNs were more effective as free drug, as an anti-tumor agent (Fig. 4). The plane SLNs did not cause cytotoxicity since the cell viability was estimated above 95%. Present results suggested that resveratrol retained its anti-tumor activity upon encapsulation into the lipid carrier. This study advocates for usefulness of resveratrol-loaded SLN in inhibiting the growth of prostate cancers.

The MTT assay was performed in PC-3 cells to investigate the concentration and time dependent cytotoxic response (% growth inhibition) of Res loaded SLNs formulations in comparison to free Res. The cell viability of phospholipid and solid lipids were both well tolerated as the lipid matrices of SLNs. Soya lecithin (natural bio-acceptable surfactant) is located mainly on SLNs surface. Consistent to what has been reported earlier (Muller *et al*., 1997), it is found that, lower/acceptable range of cytotoxicity of lipid nano-carriers as compared to polymeric nanoparticles particularly SLNs consisting lecithin. The no/feeble cytotoxicity of colloidal drug carriers are considered as better delivery vehicles to be used in *in vivo* studies. It was also noticed that nature of lipid matrix had no effect on cell viability. The Res-SLN undoubtedly

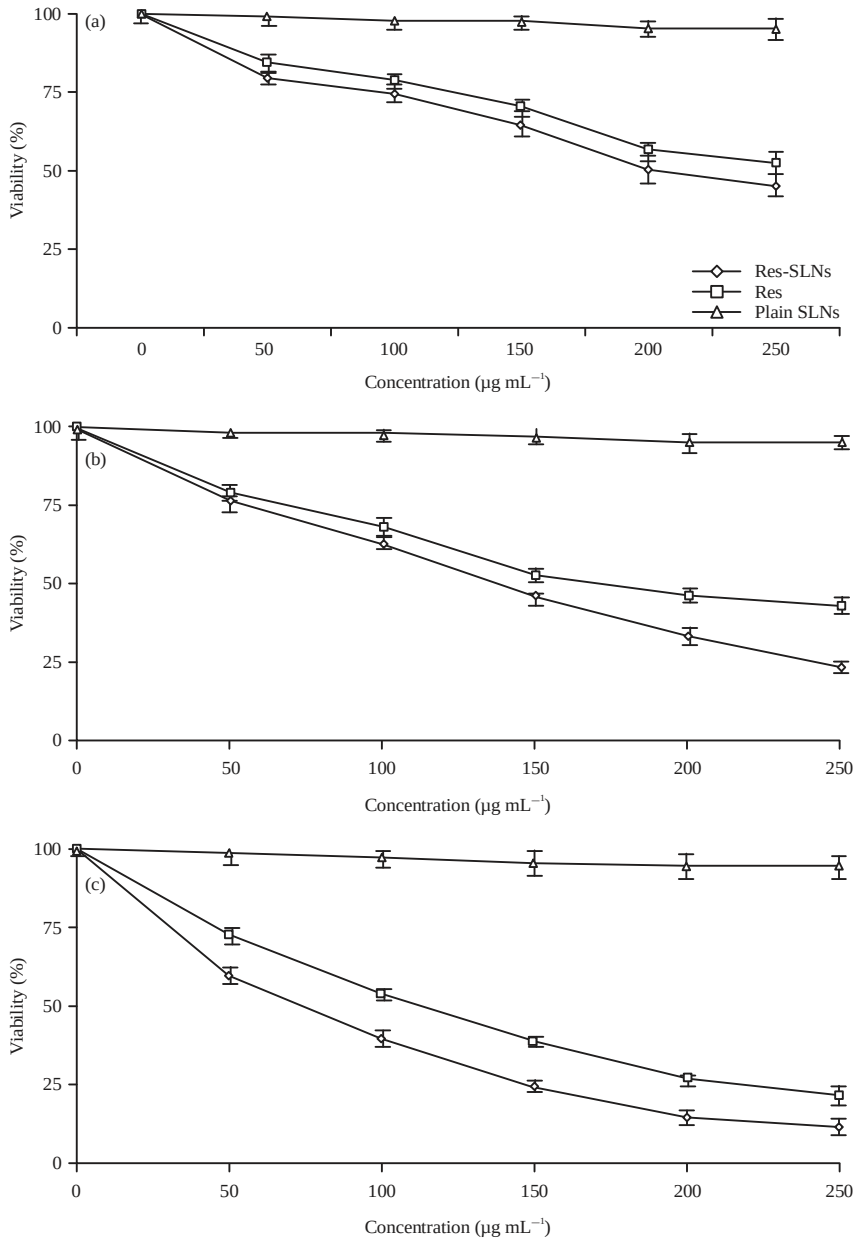

Fig. 4(a-c): Percentage cell viability of plain Res, plain SLNs and reservatrol loaded SLNs, when incubated with PC cells for (a) 24 h, (b) 48 h and (c) 72 h. Each data point represented as Mean±SD (n = 4)

suggested the significantly augmented percentage cellular inhibition or death of prostate cancer cells with the increasing concentration of Res. The inhibitory effect of free Res, Res-SLNs on PC-3 cells at or below 10 μg mL^{-1} was not seen. Also, amplified cytotoxic responses were estimated when the concentration of Res in free form or encapsulated in SLNs was increased abruptly. Nearly 100% mortality of cells was observed, when Res concentration was used in the rage from 200-250 μg mL^{-1}. It indicates the internalization of satisfactory quantity of Res within the nuclei during the incubation time of 72 h (Fig. 4c). The PC-3 cells were observed to be more sensitive to Res when encapsulated into SLNs and increased cytotoxicity was seen upon increasing the concentration (Fig. 4a-c). It may possibly be due to passive interaction and diffusion involving, which may lead to higher internalization. The greater internalization, accumulation of nanoparticles accompanied with sustained release of Res loaded onto nanoparticles in the cells could be

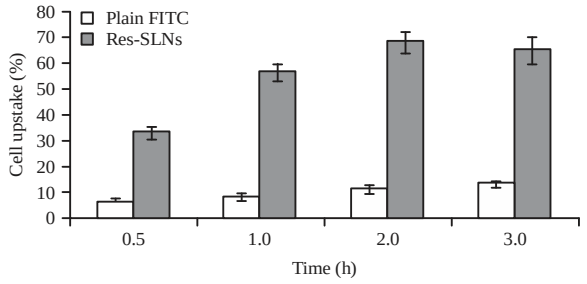

Fig. 5: Cellular uptake efficiency of plain FITC and FITC labeled SLN in PC-3 cells. Each data point represented as Mean±SD (n = 4)

responsible for augmented cytotoxicity. Therefore, a strong sensitization was achieved with Res-SLNs, which seemed to diminish the drug resistance. Further, SLNs enter the cells via passive diffusion and could be attributed to efficient cytotoxic action. The cell cytotoxicity outcomes have been complemented by the quantitative cell uptake study which revealed ~2-fold higher uptake of Res-SLN in comparison to free Res when incubated with PC-3 cells.

Cellular uptake study: The intracellular SLN delivery was followed from the first interaction between SLN-cell membrane and further uptake of SLN by PC cells. The fluorescently labeled SLN was used to examine their ability to cross the cell membrane, rate of intracellular uptake and distribution within the cells. Figure 5 depicted the rapid migration of SLN across membrane and cells have shown to taken up the significant fraction of administered dose. The green fluorescence intensity could be qualitatively assessed within cells during 15 min of the application.

Cellular uptake of Res when loaded onto SLN formulations, as the function of galactose conjugation and incubation time was evaluated on PC-3 cells using flow cytometer (C6 venturimeter, USA) (Fig. 5). The PC-3 cells were incubated with plain FITC, FITC labeled plain SLN (SLN-F) formulations. The rapid cellular localization of fluorescent SLN could be correlated with their nano-size and composition because as they are constituted with bio-acceptable and bio-degradable entities for example, solid lipids and lecithin (Miglietta *et al*., 2000). The results of this study suggested 6.2±1.4 and 33.2±1.3% cellular internalization after 0.5 h of incubation with plain FITC, SLN-F, respectively (Fig. 5). The cellular internalization was marked as 11.5±1.6 and 68.7±1.3% after 2 h incubation with plain FITC and SLN-F, respectively. The cell uptake study shows time-dependent cellular internalization of SLN and cells associated with SLNs demonstrate highest fluorescent intensity. This may be owing to passive adhesion followed by phagocytic uptake of complex (Moore *et al*., 1998; Budzynska *et al*., 2007). The internalization due to SLN-F might be owing to fluid phase endocytosis/phagocytosis mediated non-specific inter-localization. The FITC alone might non-specifically adsorb on to the surface of cells and thus emitted fluorescence signals (Schoepf *et al*., 1998) (Fig. 6). The quantitative cellular uptake studies (Fig. 5) were corroborated by the immunofluorescence assay showing photomicrographs with higher uptake of Res-SLNs in tumor cells (Fig. 6).

Assessment of nucleosomal damage: The inhibitory effects of Res and Res-loaded SLNs in the induction of cell apoptosis was assessed. The PI was used for staining nuclei of prostate cancer cells treated with either resveratrol or Res loaded SLNs (Fig. 7) showing sizeable nuclear fragmentation. However, PC cells treated with Re-SLNs showed substantially greater nuclear fragmentation depending upon Res (potential/activity) and their concentration. The conventional agarose gel electrophoresis was carried out to see an effect of treated formulations (Res and Res-SLNs) on nuclear DNA fragmentation. The DNA gel electrophoresis (Fig. 8) pattern was seen after PC cells were treated with nanoparticle formulations (res and res-SLNs).The oxidative stress in prostate cancer cells was assessed (Fig. 8) and Res and Res-SLNs for 2 h showed fragmented DNA (lane III and IV) on agarose gel in comparison to control (lane II) where, no or minimal DNA fragmentation was observed in formulation treated cells. Figure 7 and 8 demonstrated the greater DNA fragmentation with Res-SLNs (100 μg mL^{-1}) as compared to that seen with plane Res and experimental control. . These results validate of our hypothesis and confirm the role of resveratrol in increasing apoptosis in prostate cancer cells and renders protection against it.

Effect of anti-oxidants on Bcl-2 level: Considering the anti-apoptotic role of Bcl-2, it was decided to assess the relevance of this protein in conferring protection against prostate cancer when treated with resveratrol (Fig. 9). The Res and Res-SLNs showed a decrease in the bcl-2 level after PC cells were treated with resveratrol (100 μg mL^{-1}), Res-SLN and control in cell mediated reaction. The obtained apoptosis results (Fig. 9) suggest that Res and Res-SLNs treatment was given to PC cells for 18 h, which saw a significant decrease in Bcl-2 levels. The inhibited levels of the gene/protein factor of Bcl-2 family is indicative of induction prostate cancer cell apoptosis when treated with Res and Res loaded SLNs.

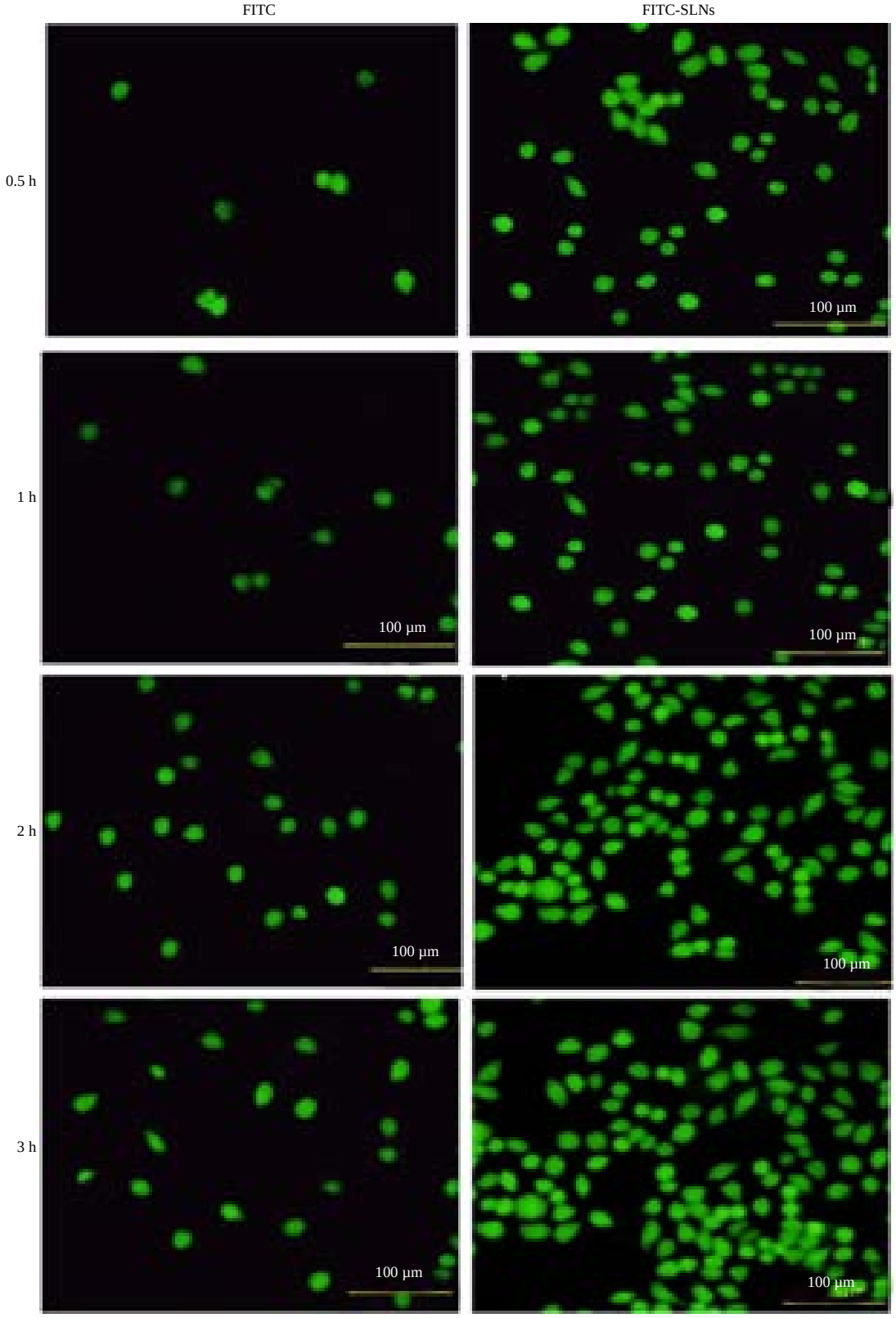

Fig. 6: Immunofluorescence assay to assess the time dependent cellular uptake of plane FITC and FITC labelled SLN by PC-3 cells

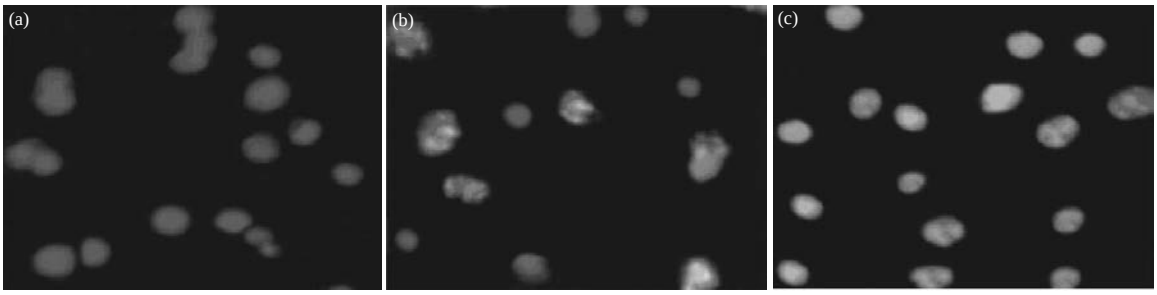

Fig. 7(a-c): Nuclear fragmentation observed after the treatment of resveratrol and resveratrol loaded solid lipid nanoparticles treated PC-3 cells. The fluorescence captured at 200x magnification

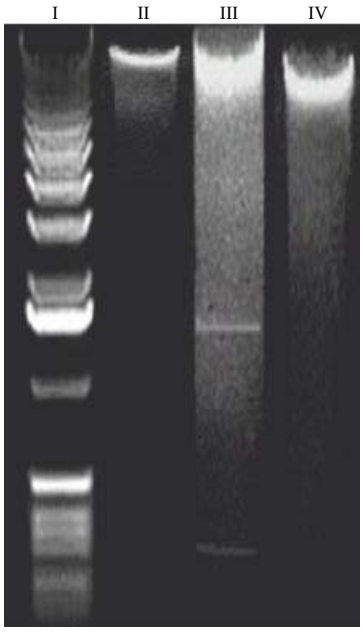

Fig. 8: Detection of DNA fragmentation to assess the programmed cell death by agarose gel electrophoresis. Lane I: Marker, Lane II: Normal PC-3 (positive control), Lane III Res-SLNs and Lane IV: Resveratrol

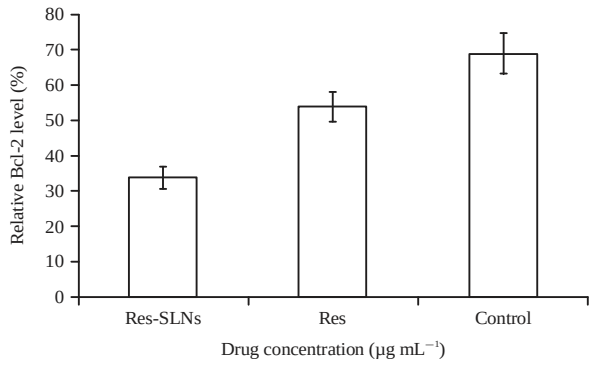

Fig. 9: Determination of relative levels of Bcl-2 (anti-apoptotic factor) after the treatment of resveratrol and Res-SLNs treatment. Results are expressed as Mean±SD (n = 6)

CONCLUSION

The present study has shown the effective and successful preparation of resveratrol loaded onto SLNs in prostate cancer therapeutics. The formulations were prepared using stearic acid and tristearin as the lipid core and phospholipid combinations of tween 80 as shell material though emulsion solvent evaporation method. The formulation parameters, such as composition of surfactant and the drug-lipid ratio were observed to influence the encapsulation of drug (resveratrol) into lipid core. Present results were indicative of minimal or no cytotoxicity shown by resveratrol-loaded SLNs, in which free drug was found effective in inducing selective apoptosis of prostate cancer. The higher accumulation of resveratrol in prostate cancer cells via SLN suggests that these nanocarriers may prove very useful for effective and targeted delivery of resveratrol to site of prostate cancer. These results are very promising considering the fact that to achieving therapeutic effect against prostate cancer, the decreased amount of resveratrol may be used. The higher efficiency in targeting and delivery, as compared to free drug, will certainly contribute in minimizing the associated adverse effects. Further, size of formulated SLN and in vitro release profile of loaded resveratrol can be further explored by different types and content of lipid materials. In conclusion, these lipid nanocarriers hold promise as a potential therapeutic agent to treat neoplastic diseases located in the prostate tissue.

ACKNOWLEDGMENT

This study was funded by a grant from Govt of China. The funders had no role in study design, data collection and analysis, decision to publish or preparation of the manuscript.

REFERENCES

Alqahtani, S. and A. Kaddoumi, 2015. Vitamin E transporters in cancer therapy. AAPS J., 17: 313-322.

Antwi, S.O., S.E. Steck, L.J. Su, J.R. Hebert and H. Zhang *et al*., 2015. Dietary, supplement and adipose tissue tocopherol levels in relation to prostate cancer aggressiveness among African and European Americans: The North Carolina-Louisiana Prostate Cancer Project (PCaP). Prostate, 75: 1419-1435.

Bishayee, A., 2009. Cancer prevention and treatment with resveratrol: From rodent studies to clinical trials. Cancer Prev. Res., 2: 409-418.

Budzynska, R., D. Nevozhay, U. Kanska, M. Jagiello, A. Opolski, J. Wietrzyk and J. Boratynski, 2007. Antitumor activity of mannan-methotrexate conjugate *in vitro* and *in vivo*. Oncol. Res., 16: 415-421.

Cain, K., S.B. Bratton and G.M. Cohen, 2002. The Apaf-1 apoptosome: A large caspase-activating complex. Biochimie, 84: 203-214.

Carlsen, M.H., B.L. Halvorsen, K. Holte, S.K. Bohn and S. Dragland *et al*., 2010. The total antioxidant content of more than 3100 foods, beverages, spices, herbs and supplements used worldwide. Nutr. J., Vol. 9. 10.1186/1475-2891-9-3.

Chandra, J., A. Samali and S. Orrenius, 2000. Triggering and modulation of apoptosis by oxidative stress. Free Radical Biol. Med., 29: 323-333.

Empl, M.T., M. Albers, S. Wang and P. Steinberg, 2015. The resveratrol tetramer r-viniferin induces a cell cycle arrest followed by apoptosis in the prostate cancer cell line LNCaP. Phytother. Res., 29: 1640-1645.

Finkel, T. and N.J. Holbrook, 2000. Oxidants, oxidative stress and the biology of ageing. Nature, 408: 239-247.

Fleshner, N.E. and L.H. Klotz, 1998. Diet, androgens, oxidative stress and prostate cancer susceptibility. Cancer Metastasis Rev., 17: 325-330.

Fraser, S.P., A. Peters, S. Fleming-Jones, D. Mukhey and M.B. Djamgoz, 2014. Resveratrol: Inhibitory effects on metastatic cell behaviors and voltage-gated Na^+ channel activity in rat prostate cancer *in vitro*. Nutr. Cancer, 66: 1047-1058.

Garcia-Ruiz, C., A. Colell, A. Morales, N. Kaplowitz and J.C. Fernandez-Checa, 1995. Role of oxidative stress generated from the mitochondrial electron transport chain and mitochondrial glutathione status in loss of mitochondrial function and activation of transcription factor nuclear factor-κB: Studies with isolated mitochondria and rat hepatocytes. Mol. Pharmacol., 48: 825-834.

Gardner, A.M., F.H. Xu, C. Fady, F.J. Jacoby, D.C. Duffey, Y. Tu and A. Lichtenstein, 1997. Apoptotic vs. nonapoptotic cytotoxicity induced by hydrogen peroxide. Free Radic Biol. Med., 22: 73-83.

Garg, N.K., S. Mangal, T. Sahu, A. Mehta, S.P. Vyas and R.K. Tyagi, 2011. Evaluation of anti-apoptotic activity of different dietary antioxidants in renal cell carcinoma against hydrogen peroxide. Asian Pac. J. Trop. Biomed., 1: 57-63.

Garg, N.K., B. Singh, G. Sharma, V. Kushwah, R.K. Tyagi, S. Jain and O.P. Katare, 2015. Development and characterization of single step self-assembled lipid polymer hybrid nanoparticles for effective delivery of methotrexate. RSC Adv., 5: 62989-62999.

Iwashita, K., M. Kobori, K. Yamaki and T. Tsushida, 2000. Flavonoids inhibit cell growth and induce apoptosis in B16 melanoma 4A5 cells. Biosci. Biotechnol. Biochem., 64: 1813-1820.

Jain, A., P. Kesharwani, N.K. Garg, K. Jain and S.A. Jain *et al*., 2015. Galactose engineered solid lipid nanoparticles for targeted delivery of doxorubicin. Colloids Surfaces B: Biointerf., 134: 47-58.

Johnson, I.T., G. Williamson and S.R.R. Musk, 1994. Anticarcinogenic factors in plant foods: A new class of nutrients? Nutr. Res. Rev., 7: 175-204.

Kobori, M., K. Iwashita, H. Shinmoto and T. Tsushida, 1999. Phloretin-induced apoptosis in B16 melanoma 4A5 cells and HL60 human leukemia cells. Biosci. Biotechnol. Biochem., 63: 719-725.

La Vecchia, C., A. Altieri and A. Tavani, 2001. Vegetables, fruit, antioxidants and cancer: A review of Italian studies. Eur. J. Nutr., 40: 261-267.

Lennon, S.V., S.J. Martin and T.G. Cotter, 1991. Dose-dependent induction of apoptosis in human tumour cell lines by widely diverging stimuli. Cell Prolif., 24: 203-214.

Lin, H., J.P. Lu, P. Laflamme, S. Qiao and B. Shayegan *et al*., 2010. Inter-related *in vitro* effects of androgens, fatty acids and oxidative stress in prostate cancer: A mechanistic model supporting prevention strategies. Int., 37: 761-766.

Lowry, O.H., N.J. Rosebrough, A.L. Farr and R.J. Randall, 1951. Protein measurement with the Folin phenol reagent. J. Biol. Chem., 193: 265-275.

Mathiasen, I.S. and M. Jaattela, 2002. Triggering caspase-independent cell death to combat cancer. Trends Mol. Med., 8: 212-220.

Miglietta, A., R. Cavalli, C. Bocca, L. Gabriel and M.R. Gasco, 2000. Cellular uptake and cytotoxicity of Solid Lipid Nanospheres (SLN) incorporating doxorubicin or paclitaxel. Int. J. Pharm., 210: 61-67.

Mitani, T., N. Harada, S. Tanimori, Y. Nakano, H. Inui and R. Yamaji, 2014. Resveratrol inhibits hypoxia-inducible factor-1α-mediated androgen receptor signaling and represses tumor progression in castration-resistant prostate cancer. J. Nutr. Sci. Vitaminol., 60: 276-282.

Mohanty, S.K., K. Malappa, A. Godavarthi, B. Subbanarasiman and A. Maniyam, 2014. Evaluation of antioxidant, *in vitro* cytotoxicity of micropropagated and naturally grown plants of *Leptadenia reticulata* (Retz.) Wight & Arn.-an endangered medicinal plant. Asian Pac. J. Trop. Med., 7: S267-S271.

Moore, A., J.P. Basilion, E.A. Chiocca and R. Weissleder, 1998. Measuring transferrin receptor gene expression by NMR imaging. Biochim. Biophys. Acta (BBA)-Mol. Cell Res., 1402: 239-249.

Muller, R.H., D. Ruhl, S. Runge, K. Schulze-Forster and W. Mehnert, 1997. Cytotoxicity of solid lipid nanoparticles as a function of the lipid matrix and the surfactant. Pharm. Res., 14: 458-462.

Pathak, S.K., R.A. Sharma, W.P. Steward, J.K. Mellon, T.R. Griffiths and A.J. Gescher, 2005. Oxidative stress and cyclooxygenase activity in prostate carcinogenesis: Targets for chemopreventive strategies. Eur. J. Cancer, 41: 61-70.

Schoepf, U., E.M. Marecos, R.J. Melder, R.K. Jain and R. Weissleder, 1998. Intracellular magnetic labeling of lymphocytes for *in vivo* trafficking studies. Biotechniques, 24: 642-646, 648-651.

Tjalma, W.A., J.J. Weyler, J.J. Bogers, C. Pollefliet and M. Baay *et al*., 2001. The importance of biological factors (bcl-2, bax, p53, PCNA, MI, HPV and angiogenesis) in invasive cervical cancer. Eur. J. Obstet. Gynecol. Reprod. Biol., 97: 223-230.

Torricelli, P., P. Ricci, B. Provenzano, A. Lentini and C. Tabolacci, 2011. Synergic effect of α-tocopherol and naringenin in transglutaminase-induced differentiation of human prostate cancer cells. Amino Acids, 41: 1207-1214.

Ueda, N. and S.V. Shah, 1992. Endonuclease-induced DNA damage and cell death in oxidant injury to renal tubular epithelial cells. J. Clin. Invest., 90: 2593-2597.

Walle, T., 2011. Bioavailability of resveratrol. Ann. N. Y. Acad. Sci., 1215: 9-15.

Wang, I.K., S.Y. Lin-Shiau and J.K. Lin, 1999. Induction of apoptosis by apigenin and related flavonoids through cytochrome c release and activation of caspase-9 and caspase-3 in leukaemia HL-60 cells. Eur. J. Cancer, 35: 1517-1525.

Zimmermann, K.C., C. Bonzon and D.R. Green, 2001. The machinery of programmed cell death. Pharmacol. Ther., 92: 57-70.